Available online at www.sciencedirect.com
ScienceDirect
Atmospheric Environment 40 (2006) 7579–7588
ATMOSPHERIC ENVIRONMENT
www.elsevier.com/locate/atmosenv

Role of the binary H_2SO_4–H_2O homogeneous nucleation in the formation of volatile nanoparticles in the vehicular exhaust

Hua Du*, Fangqun Yu

Atmospheric Sciences Research Center, State University of New York at Albany Albany, NY 12203, USA

Received 17 October 2005; received in revised form 23 May 2006; accepted 1 July 2006

Abstract

High concentration of volatile nanoparticles (NPs) formed in vehicular exhaust may lead to adverse health effects, and a clear understanding of the nucleation mechanisms of these particles remains to be achieved. We investigate the role of H_2SO_4–H_2O binary homogeneous nucleation (BHN) in the formation of NPs in the diluting vehicular exhaust, using a recently developed kinetic H_2SO_4–H_2O BHN model suitable for studying the nucleation process in rapidly diluting exhaust. For the vehicles running on the fuel with fuel sulfur content (FSC) of ~330 ppm we found that BHN may significantly contribute to the NP formation, especially when the ambient temperature is low and the relative humidity is high. Our simulations show that BHN rate is very sensitive to FSC and sulfur to sulfuric acid conversion efficiency (ε_s). For ε_s value of 1%, BHN is negligible under typical conditions when FSC is $<\sim$100 ppm. However, NP formation via BHN may still be significant if $\varepsilon_s > \sim$4% even after FSC is reduced to below ~50 ppm. The sensitivities of NP formation via BHN to key factors (including ambient temperature and relative humidity, FSC, ε_s and the soot number concentration) are presented.

Keywords: Nanoparticles; Fuel sulfur content; Vehicle exhaust; Kinetic quasi-unary nucleation model

1. Introduction

Motor vehicles are known to be a significant source of NPs that may cause adverse health effect due to their high number concentration and lung-deposition efficiency (Donaldson et al., 1998). It is important to have a clear understanding of the mechanisms controlling the formation of these NPs. Such an understanding is not only critical to help establish criteria for engine design, operation, after-treatment, fuel and lubricating oil compositional modifications that would effectively reduce NP emissions, but also is important to develop NP emission inventories.

Only sulfuric acid is likely to become super-saturated enough for homogeneous nucleation during diluting vehicular exhaust (Tobias et al., 2001); and various versions of the classical H_2SO_4–H_2O BHN theory have been applied to study the new particle formation in diluting engine exhaust (Baumgard and Johnson, 1996; Shi and Harrison, 1999; Kim et al., 2002; Zhang and Wexler, 2004). However, there exists a limitation

*Corresponding author. Tel.: +1 518 437 8726; fax: +1 518 437 8758.
E-mail addresses: huadu@asrc.cestm.albany.edu (H. Du), yfq@asrc.cestm.albany.edu (F. Yu).

1352-2310/$ - see front matter © 2006 Elsevier Ltd. All rights reserved.
doi:10.1016/j.atmosenv.2006.07.012

in using classical BHN theory to calculate the particle formation rates in vehicular exhaust. The classical BHN theory assumes that steady-state equilibrium distribution of critical clusters is achieved instantaneously at given H_2SO_4 concentration ($[H_2SO_4]$), temperature (T) and relative humidity (RH). The classical BHN model cannot keep track of the cluster distributions in the rapidly diluting engine exhaust due to the dramatic changes in T, RH and $[H_2SO_4]$ (and resulting size of critical clusters) when fresh engine exhaust mixes with ambient air, the cluster distributions in the rapidly diluting engine exhaust are likely to change quickly and the classical BHN model cannot keep track of these changes properly. Recently Yu (2005, 2006) showed that the BHN of H_2SO_4–H_2O can be treated as quasi-unary nucleation of H_2SO_4 in equilibrium with H_2O vapor and developed a kinetic H_2SO_4–H_2O nucleation model. This kinetic model can keep track of the clusters of all sizes in the diluting exhaust experiencing rapid changes in T, RH and $[H_2SO_4]$, and thus is a more robust method to study engine-generated NPs.

The main objective of this study is to investigate, with the recently developed kinetic H_2SO_4–H_2O nucleation model, the conditions in which the BHN is significant in engine exhaust. We first re-analyze the laboratory measurements of Shi and Harrison (1999), focusing mainly on the effect of the T and RH of the dilution air on the homogeneous nucleation rates. Then, we investigate the key parameters controlling the H_2SO_4–H_2O homogeneous nucleation rates in the vehicular exhaust experiencing continuous dilution in the atmosphere.

2. Kinetic H_2SO_4–H_2O quasi-unary nucleation (QUN) model

The H_2SO_4–H_2O BHN theory has been intensively studied in the last few decades and a number of updates to the classical BHN theory have been made in the past (Doyle, 1961; Jaecker-Voirol et al., 1987; Noppel et al., 2002). In this study we use a kinetic method to investigate the NP formation because of rapid changes in the T, RH of engine exhaust and $[H_2SO_4]$ during the exhaust continuous dilution.

The kinetic QUN model (Yu, 2005, 2006) simulates the evolution of cluster size spectra explicitly, which are necessary when the ambient conditions change rapidly. It has been demonstrated that the nucleation rates predicted by the kinetic QUN model (Yu, 2005, 2006) are in good agreement with recent experimental BHN data. The detailed description of the kinetic QUN model is given in Yu (Yu, 2005, 2006). Here, the physical basis and the key assumptions of the QUN model are summarized briefly:

(1) At given T and RH, the sulfuric acid clusters of various sizes are in equilibrium with water and their average compositions (i.e. the number of H_2O molecules i_b in a cluster containing i_a H_2SO_4 molecules) can be approximated using the most stable compositions (Yu, 2005).
(2) The binary H_2SO_4–H_2O nucleation is controlled by the growth/shrink of $(H_2SO_4)_{i_a}(H_2O)_{i_b}$ clusters (named i_a-mers thereafter) through the uptake/evaporation of H_2SO_4 molecules. The cluster forward/growth rate (β_{i_a}) is the kinetic collision rate of the hydrated monomers with i_a-mers, and the reverse/evaporation rate (γ_{i_a}) is the escape frequency of H_2SO_4 molecules from i_a-mers calculated using the Kelvin equation. The intersection points of β_{i_a} and γ_{i_a} curves are those where the critical clusters are located and the properties of the critical clusters (number of the sulfuric acid molecules i_a^*, radius r^*, the acid mole fraction x^*, etc.) are simulated explicitly.
(3) When the compositions, β_{i_a} and γ_{i_a} for i_a-mers are known, the time-dependent cluster number concentration size distributions $(n_{i_a}(t))$ can be obtained by solving the following set of the differential equations:

$$\frac{dn_{i_a}}{dt} = \delta_{i_a-1,1}\beta_{i_a-1}n_{i_a-1} - \gamma_{i_a}n_{i_a} - \beta_{i_a}n_{i_a} + \gamma_{i_a+1}n_{i_a+1} + \frac{1}{2}\sum_{k=2}^{i_a-2} k_{i_a-k,k}n_{i_a-k}n_k - \sum_{j=2}^{\infty} k_{i_a,j}n_{i_a}n_j - \sqrt{\frac{kT}{2\pi m_{i_a}}}A_p n_{i_a}, \quad i_a \geqslant 2, \tag{1}$$

$$\frac{dn_1}{dt} = P - \sum_{i_a=1}^{\infty}\beta_{i_a}n_{i_a} + 2\gamma_2 n_2 + \sum_{i_a=3}^{\infty}\gamma_{i_a}n_{i_a} - \sqrt{\frac{kT}{2\pi m_1}}A_p n_1, \tag{2}$$

where P is the production rate of sulfuric acid molecules ($P = 0\,\mathrm{cm^{-3}\,s^{-1}}$ in this study). $k_{i,j}$ is the coagulation kernel. $\delta_{i_a-1,1} = 1$ when $i_a > 2$ and $= 0.5$ when $i_a = 2$. A_p is the total surface area associated with soot particles (assumed to be 50 nm in diameter) in the exhaust and entrained background aerosols, k is Boltzmann's constant, and m_{i_a} is the mass of i_a-mers.

3. Modeling results

3.1. NPs formation in the two-stage laboratory dilution tunnel

Shi and Harrison (1999) investigated the NP formation in the diesel exhaust experiencing two-stage dilution in the laboratory. Their experiments have shown a considerable sensitivity of the NP production to the dilution conditions. Here we apply the kinetic QUN model to study in detail the BHN in laboratory conditions. The study is divided into case (a) and case (b). The parameters (T, RH, dilution ratio DR, residence time for both stages, initial sulfuric acid vapor concentration ($[H_2SO_4]_{initial}$) and soot concentration) for case (a) are taken from the laboratory study (Shi and Harrison, 1999). The only change in parameters for case (b) is that the T of first-stage dilution air is decreased by 12 K. Here we treat all volatile particles with diameter >3 nm as nucleated particles. The condensation of organic species on the nucleated particles was not considered in the current study as the main focus of this paper is on the number of particles formed via BHN under different conditions. Organic compounds are known to contribute to the growth of the nucleated particles (and thus their sizes) but their effect on the number of particles nucleated appears to be limited though further research is needed. In order to compare simulated size distributions with those measured, the condensation of organics has to be included in the model which will require information about the types of organic compounds involved in the condensation and their properties (vapor pressure, surface tension, etc.).

We start the simulation from the beginning of first-stage dilution where the raw exhaust was just diluted by a factor of 9.9. $[H_2SO_4]_{initial}$ in the first-stage dilution tunnel is $1.14 \times 10^{12}\,\mathrm{cm^{-3}}$. Fig. 1 shows β_{i_a} and γ_{i_a} of i_a-mers at different time points in the first-stage dilution tunnel for cases (a) and (b). In case (a), the diluted exhaust temperature (T_e) is 321 K and relative humidity (RH_e) is 16.2% (3). In case (b), $T_e = 310\,\mathrm{K}$, $RH_e = 17.3\%$.

According to Figs. 1(a) and (b), γ_{i_a} decreases rapidly as i_a increases, especially when i_a is small, and is very sensitive to T_e and RH_e but independent of $[H_2SO_4]$. β_{i_a} is proportional to $[H_2SO_4]$ and the effect of T_e and RH_e on β_{i_a} is small. β_{i_a} decreases as time elapses as a result of decrease in $[H_2SO_4]$ due to

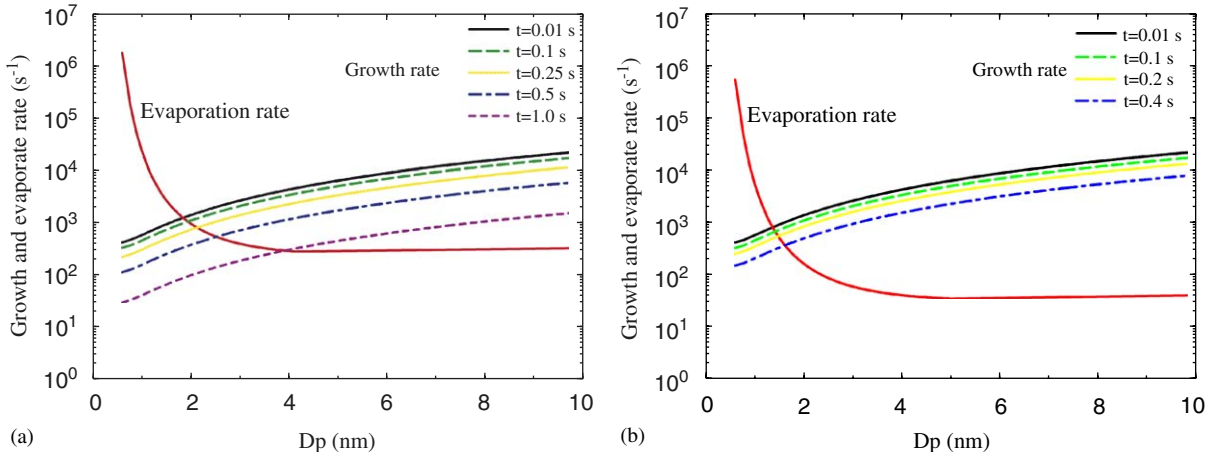

Fig. 1. Growth rates (β_{i_a}) and evaporation rates (γ_{i_a}) of $(H_2SO_4)_{ia}(H_2O)_{ib}$ clusters for (a) $T_e = 321\,\mathrm{K}$, $RH_e = 16.2\%$ and (b) $T_e = 310\,\mathrm{K}$, $RH_e = 17.3\%$. $[H_2SO_4]_{initial} = 1.14 \times 10^{12}\,\mathrm{cm^{-3}}$ in both cases. β_{i_a} decreases with $[H_2SO_4]_{initial}$ while γ_{i_a} remains unchanged due to the fixed T_e and RH_e. The intersection point of curves β and γ at each time point is where cluster critical size locates. Cluster critical sizes increases with time, implying the decrease in nucleation rate.

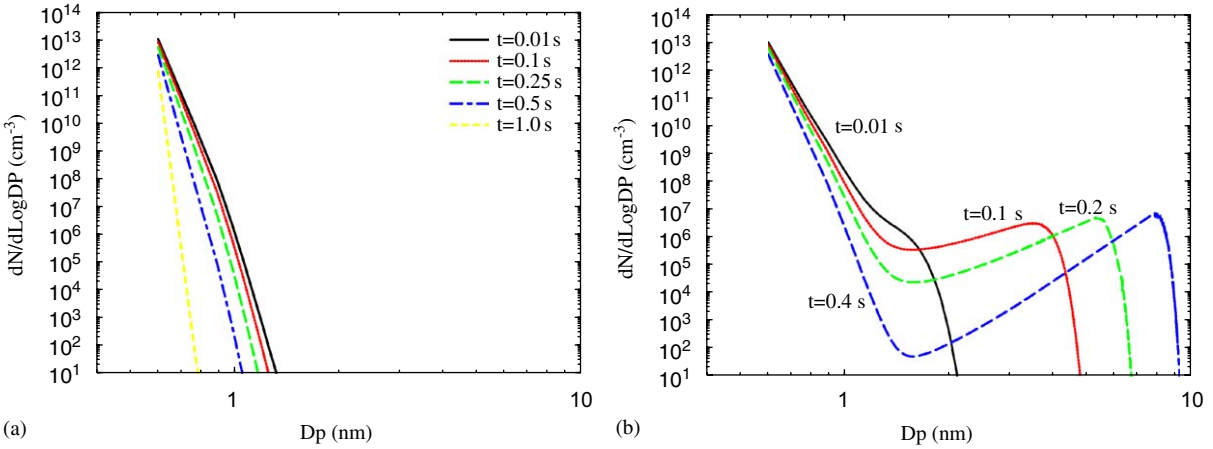

Fig. 2. Evolution of NP size distributions in the first-stage dilution tunnel for (a) $T_e = 321\,K$, $RH_e = 16.2\%$ and (b) $T_e = 310\,K$, $RH_e = 17.3\%$. $[H_2SO_4]_{initial} = 1.14 \times 10^{12}\,cm^{-3}$ in both cases. Soot concentration is $3.0 \times 10^6\,cm^{-3}$ in the first dilution stage. No particles grow bigger than the detectable size (~3 nm) based on the two-stage experimental conditions (Shi and Harrison, 1999) in Fig. 2(a) while a clear nuclei-mode appears ~8 nm in case (b), suggesting that BHN may lead to significant NPs under favorable laboratory conditions.

nucleation process and soot scavenging. The intersection points of β_{ia} and γ_{ia} curves correspond to the sizes of critical clusters. Clusters smaller than critical clusters tend to evaporate while clusters larger than critical clusters tend to grow.

We solved Eqs. (1) and (2) using values of β_{ia} and γ_{ia} shown in Fig. 1 to obtain the evolution of cluster size spectra. Fig. 2(a) shows the cluster size distributions at $t = 0.01$, 0.1, 0.25, 0.5 and 1.0 s for case (a). Few clusters grow beyond 1.0 nm before 0.01 s, while cluster size distributions begin to shift backwards as a result of evaporation since then. Evaporation of small clusters occurs mainly due to the decrease in $[H_2SO_4]$ associated with soot scavenging.

Obviously, no NPs can form via BHN under Shi and Harrison's (1999) experimental conditions based on our simulation. The maximum nucleation rate estimated based on an earlier version of the classical BHN theory (Kulmala et al., 1998; Shi and Harrison, 1999) was much higher than our simulations but was still ~60 times smaller than the observed value. The difference in the predicted nucleation rates is not surprising because the kinetic model used in this study is quite different from the classical BHN theory used in Shi and Harrison's estimation. A detailed comparison of QUN and BHN has been given in Yu (2005, 2006). It should also be noted that the estimation given by Shi and Harrison (1999) was the maximum value because the scavenging of precursor molecules and small clusters by soot particles was not considered.

Yu (2001) has shown that ion-mediated nucleation mechanism may explain the observed NPs if the concentration of chemiions in the raw exhaust can reach $1.5 \times 10^8\,cm^{-3}$. While nucleation on ions is thermodynamically more favorable than binary nucleation of H_2SO_4–H_2O, the number of NPs formed via ion nucleation is limited by the availability of ions. Nevertheless, the ion nucleation does not exclude the possibility of homogeneous nucleation and the contribution of BHN in certain circumstances still maybe significant, as indicated in Fig. 2(b), which shows that a lower first dilution stage exhaust temperature significantly reduces the cluster evaporation rates (see Fig. 1(b)) and thus enhances the nucleation. A clear nucleation mode with the mean size of ~3.5 nm emerges at $t = 0.1$ s and grows rapidly to a larger size. The minimum in the size distributions around 1.5 nm is where the critical size locates.

Since T and RH of dilution air (T_D and RH_D) have significant effects on NP formation in laboratory conditions as shown in the above simulations, we further investigate the sensitivities of NP formation to T_D and RH_D, aiming at understanding the laboratory conditions in which BHN could make a significant contribution to NPs production. For simplicity, we assume the same T_D and RH_D for both dilution stages with other parameters the same as case (a).

Fig. 3 illustrates the number concentration of particles larger than 3 nm in diameter ($N_{d>3\,nm}$) at $t = 1.8$ s as a function of T_D at three different RH_D

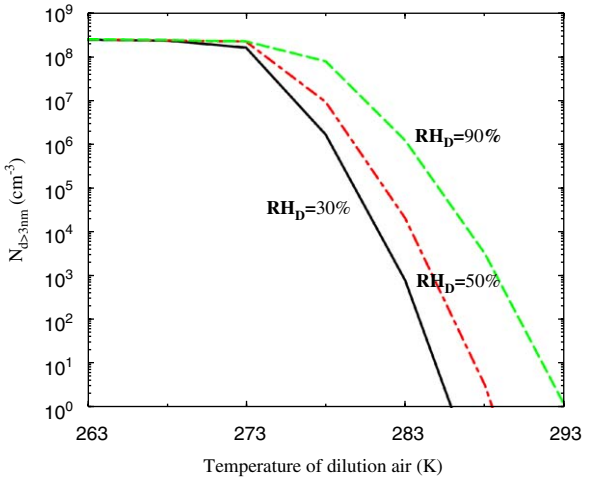

Fig. 3. Influences of dilution air temperature (T_D) on $N_{d>3\,nm}$ (at $t = 1.8$ s) at three-selected RH_D (30%, 50% and 90%). $[H_2SO_4]_{initial}$ and soot number concentration are 1.14×10^{12} and $3.0 \times 10^6\,cm^{-3}$, respectively. $N_{d>3\,nm}$ is more sensitive to RH_D under high T_D conditions than in low T_D conditions due to coagulation-related NP number limitation.

(30%, 50% and 90%). It shows that NPs production via BHN can be significant under a wide range of T_D and RH_D in laboratory conditions. The sensitivities of $N_{d>3\,nm}$ to T_D and RH_D become negligible when $T_D < \sim 273$ K because $N_{d>3\,nm}$ is coagulation limited. Larger than 90% of RH_D is needed in order to have obvious NP production via BHN ($N_{d>3\,nm} > \sim 1000\,cm^{-3}$) if T_D is $> \sim 288$ K.

Our simulations indicate that BHN can lead to significant NP particle formation under favorable laboratory conditions, especially when T_D is low. In addition to T_D and RH_D, other factors affecting the nucleation include the $[H_2SO_4]$ in the exhaust (a function of FSC and ε_s), dilution ratio, residence time and soot particle concentrations. Some of these factors are addressed in the next section.

3.2. NPs formation in the vehicular exhaust diluting in the atmosphere

Unlike two-stage dilution process, vehicular exhaust experiences continuous dilution in the real atmosphere that leads to rapidly continuous changes of T_e, RH_e and $[H_2SO_4]$ in the exhaust. Such rapid changes would thermodynamically affect the physical properties, growth and evaporation rates of each cluster, and thus impact NP formation in vehicular exhaust.

Appropriate characterization of the dilution profile of vehicular exhaust is critical because it delineates the continuous evolution of T_e and RH_e, which affects cluster evaporation rates, and $[H_2SO_4]$, which impacts cluster growth rates. Laboratory and field studies (Kittelson et al., 1988; Kim et al., 2001; Shi et al., 2002) indicate a rapid dilution near the tailpipe within a few seconds. Dilution ratio as a function of plume age (i.e. time elapsed since the exhaust left the tailpipe) used in this study was obtained using the nonlinear regression of experimental data of Kittelson et al. (1988). The equation for the dilution ratio has been obtained in the form of $DR = 1.0 + 700 \times t^{1.413}$ ($t \leqslant 1$ s) (see Fig. S1 in Supporting information).

The initial $[H_2SO_4]$ in exhaust before continuous dilution is a function of FSC and ε_s (see Appendix (1) in Supporting information) and is proportional to ε_s when FSC is fixed. As far as we know, neither direct measurements nor chemical modeling of ε_s for motor engines is available in the literature. It is expected that ε_s depends on engine types, operation conditions and exhaust treatment systems. Evidences indicate that the change of T in catalytic converters appears to affect ε_s. In contrast to the lack of study of ε_s in motor engine exhaust, there exist extensive investigations of ε_s in jet engine exhaust (Lukachko et al., 1998). Direct measurements and chemical simulations indicate that ε_s for jet engine can range from 0.1% to 10% (Lukachko et al., 1998; Kawa et al., 1999). ε_s is assumed to be 1.0% in our baseline study and sensitivity of results to ε_s will be presented.

Due to the wide possible ranges of key parameters (T, RH, FSC, ε_s and soot concentration), we first present the time-dependent evolution of cluster size distribution for a baseline scenario. Then, the sensitivity study of NP formation to various key parameters will be given. The values of the key input parameters used in the simulations for both the baseline scenario and sensitivity study are given in Table 1. The temperature and relative humidity of raw exhaust at the tailpipe exit are assumed to be 373 K and 0.033%, respectively. For the time scale we studied here (plume age $\leqslant 1$ s), the effect of background aerosols on condensation of H_2SO_4 and scavenging of newly formed particles is not important. However, such effect may become important in far wake when the plumes are transported further away from roads.

3.2.1. Baseline scenario

The exhaust T and RH rapidly approach ambient levels as exhaust mixes with ambient air (Fig. S2(a)

Table 1
Parameters used in baseline case and sensitivity study

Parameters	Baseline case	Sensitivity study
Ambient air temperature (T_a, in K)	283.15	263.15–303.15
Ambient air relative humidity (RH_a, in %)	60	20–80
Soot particle concentration (cm^{-3})	1.0^7	1.0^4–1.0^8
Fuel sulfur content (FSC, in ppm)	330	0–400
Sulfur conversion efficiency (ε_s, in %)	1	0.1–10.0

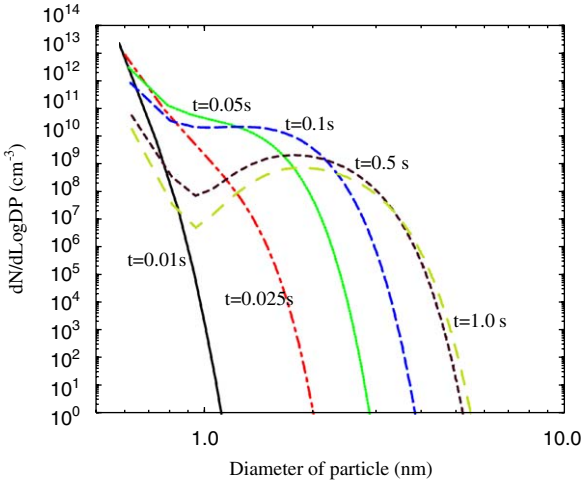

Fig. 4. Evolution of cluster/NP size distributions as the exhaust dilutes in the atmosphere for the baseline scenario. T_a and RH_a are 283 K and 60%, respectively. FSC and soot number concentration are 330 ppm and $1.0\times10^7\,cm^{-3}$, respectively. Particles grow bigger and their number concentrations increase with time while the number concentrations of smaller clusters decreases as they either grow into larger clusters or evaporate into smaller clusters.

in supporting information). Such change in exhaust T and RH leads to rapid nucleation of small clusters as a result of super-saturation of H_2SO_4, causing the continuous change in cluster critical size (Fig. S2(b) in supporting information).

Fig. 4 shows size distributions of NPs in the plumes of different ages ($t = 0.01$, 0.025, 0.05, 0.1, 0.5 and 1.0 s). $N_{d>3\,nm}$ increases from 0 at $t = 0.01$ s to $10^6\,cm^{-3}$ at $t = 0.2$ s, indicating a rapid NPs growth within 0.2 s of plume age (also see Fig. S3 in Supporting information). The decrease in the number concentration of clusters with diameter ~0.8 nm at $t > 0.1$ s is largely due to evaporation. The decrease in the monomer concentration and the increase in $N_{d>3\,nm}$ are the result of the condensation of H_2SO_4 vapors onto larger NPs and dilution.

3.2.2. Sensitivity study of different parameters

In baseline scenario, we showed NP production in vehicular exhaust in terms of the cluster size evolution mainly to visualize the evolution of volatile NP and understand the physical processes associated with NP formation and evolution in a given ambient condition. In the following sections, we will show how different parameters impact NP production and the significance of such influences. We also provide information on vehicle emission index of the NP (EI, in $\#\,kg^{-1}$ fuel) (see Appendix (2) in Supporting information). For the simulations presented below with regard to the sensitivity of NP formation to a certain parameter, we use baseline values for other parameters unless otherwise indicated.

3.2.2.1. Effects of T_a and RH_a. Fig. 5 illustrates $N_{d>3\,nm}$ as a function of T_a at four RH_a at plume age of 1 s. The corresponding EIs are indicated as well. It shows that NPs formation in vehicular exhaust via BHN is significant under wide ranges of ambient temperature and relative humidity. More particles are formed at lower T_a and higher RH. The effect of RH_a on $N_{d>3\,nm}$ is more significant under high T_a conditions. Under favorable conditions, $N_{d>3\,nm}$ at plume age of 1 s can reach $10^6\,cm^{-3}$ which corresponds to an EI of $\sim10^{16}\,\#\,kg^{-1}$ fuel. Kittelson et al. (2004) showed that on-road particle NP EIs on two freeways of Minnesota are in the range of $\sim2.2-11\times10^{15}\,\#\,kg^{-1}$ fuel for a gasoline-dominated vehicle fleet in wintertime conditions with T_a of 274–286 K, RH_a of 40–60% and FSC of 330 ppm. On-road particle NP EI of around $8.3\times10^{15}\,\#\,kg^{-1}$ fuel has been reported for Helsinki metropolitan area, Finland (Yli-Tuomi et al., 2005). Our simulations indicate that BHN may explain these observed high vehicular NP EIs.

3.2.2.2. Effects of FSC. Fig. 6 shows $N_{d>3\,nm}$ at plume age of 1 s as a function of FSC at six ambient conditions. We assume ε_s (1.0% in this case) does not change with FSC. Our kinetic model predicts strong sensitivity of H_2SO_4–H_2O nucleation rate to FSC. For example at $T_a = 298$ K and $RH_a = 80\%$, the nucleation rate decreases by a factor of $\sim10^4$

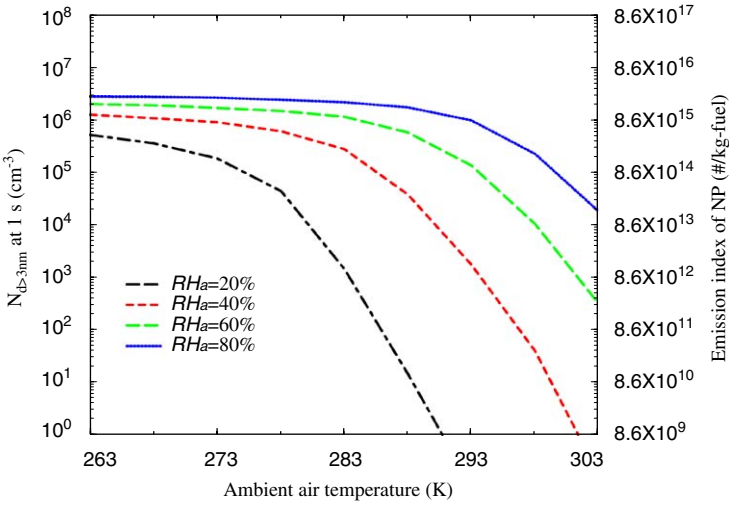

Fig. 5. Effects of ambient temperature (T_a) on $N_{d>3\,nm}$ at exhaust plume age of 1 s and the corresponding NP emission index at four RH_a. The values of other parameters (see Table 1) are the same as those in the baseline case.

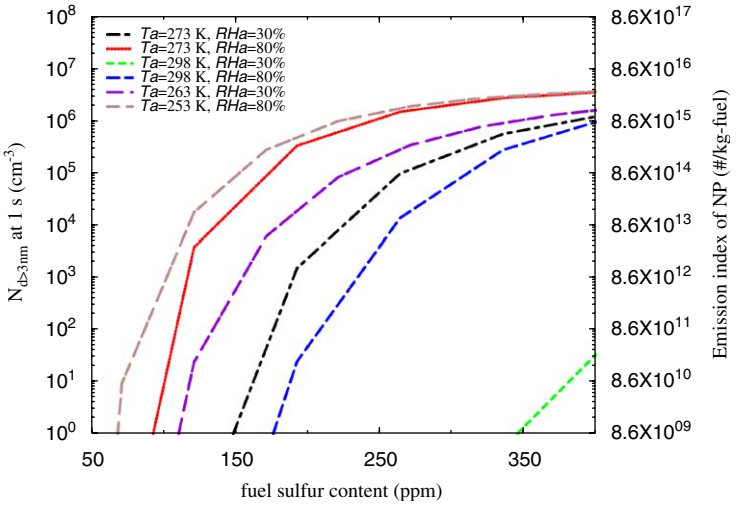

Fig. 6. Effects of FSC on $N_{d>3\,nm}$ (at $t = 1$ s) and NP emission index at six atmospheric conditions. The values of other parameters (see Table 1) are the same as those in the baseline case.

when FSC decreases from 400 to 200 ppm. When FSC <100 ppm, H_2SO_4–H_2O nucleation is very small in all typical ambient conditions. This indicates that in the states like California in which FSC $<\sim30$ ppm or in the future when fuel with ultra-low sulfur content (FSC <15 ppm) is used, the contribution of binary H_2SO_4–H_2O homogenous nucleation to new NP formation is negligible if ε_s does not change with FSC. In such cases, the observations of new NP formation in the exhaust of engines running on ultra-low sulfur fuel (FSC $<\sim15$ ppm) may indicate the involvement of other species such as ions (Yu, 2001), organics, metal or ammonia.

3.2.2.3. Effects of ε_s. Fig. 7 illustrates $N_{d>3\,nm}$ at 1 s of plume age as a function of ε_s in five atmospheric conditions. With a given FSC, the initial [H_2SO_4] in exhaust is proportional to ε_s. From Fig. 7 we could see that $N_{d>3\,nm}$ is very sensitive to ε_s, especially when ε_s is small. $N_{d>3\,nm}$ increases by $\sim10^6$ when ε_s increases from 1.5% to 4.0% for the case of 100 ppm of FSC. Thus, it is clear that ε_s is a critical parameter controlling NPs production in exhaust.

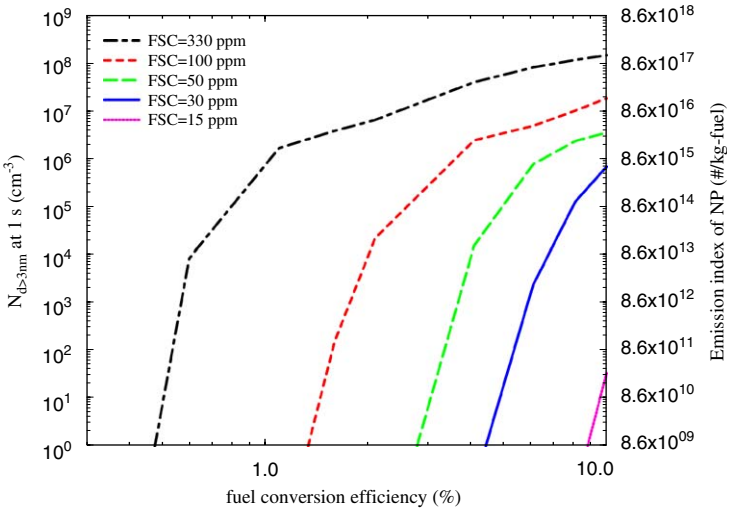

Fig. 7. Influence of ε_s on $N_{d>3\,\mathrm{nm}}$ (at $t = 1$ s) and NP emission indexes at five FSCs. The values of other parameters (see Table 1) are same as those in baseline cases.

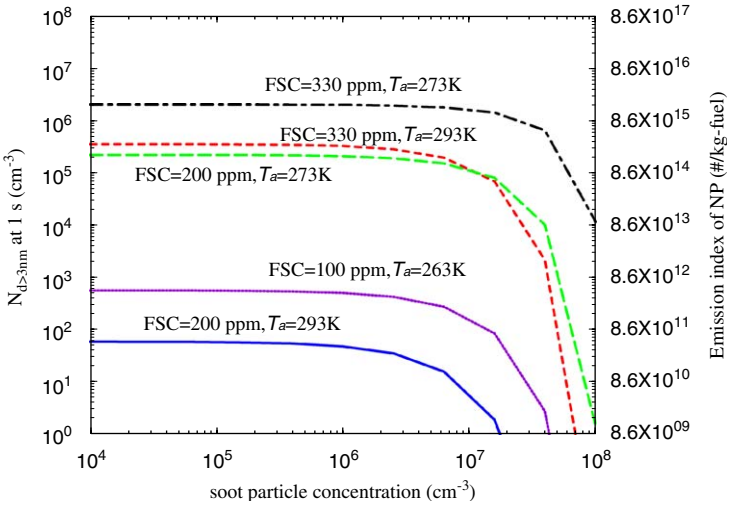

Fig. 8. Effects of soot particle number concentration on $N_{d>3\,\mathrm{nm}}$ (at $t = 1$ s) and NP emission index at five conditions. The values of other parameters (see Table 1) are same as those in baseline case.

However, as we mentioned earlier, no direct studies of ε_s for motor vehicles are available. Since different vehicles have different catalytic converters, engine designs and operation conditions, it is reasonable to expect a range of ε_s for vehicles running on roadways. Obviously, more studies on ε_s for vehicles and the parameters affecting ε_s should be carried out. Since catalytic converters may play an important role in oxidizing sulfur into sulfuric acid, future development of catalytic converter should assess its oxidizing capacity as increase in ε_s may offset the effect of FSC reduction on new NP formation.

3.2.2.4. Effects of soot scavenging. Fig. 8 illustrates $N_{d>3\,\mathrm{nm}}$ as a function of soot concentration at five conditions. Soot scavenging effect is small when soot concentration is $<\sim 1.0\times10^7\,\mathrm{cm}^{-3}$ but is significant when soot concentration is $>\sim 1.0\times10^7\,\mathrm{cm}^{-3}$. For the conditions investigated here, a reduction of soot particle concentration from 10^8 to $10^7\,\mathrm{cm}^{-3}$ increases the NP formation via homogeneous nucleation by up to 5five orders of magnitude. This is consistent with some measurements which indicate that a reduction in soot concentration as a result of cleaner modern engines

or of using a particulate filter actually leads to an increase in volatile NP emissions (Bagley et al., 1996; Graves, 1999). Nevertheless, our simulations suggest that the effect of soot emission reduction on volatile NP formation is limited after the soot concentration in the raw exhaust is reduced below $\sim 10^7\,cm^{-3}$.

4. Summary and discussion

The main objective of this study is to investigate the conditions, both in laboratory and real atmosphere, in which significant NP production via BHN in vehicular exhaust can be observed, using a recently developed kinetic QUN model which agrees well with experimental binary nucleation results. Firstly, we carried out the simulations on two-stage laboratory dilutions and found out that NP formation via BHN may become significant under favorable laboratory conditions, especially when T of first-stage dilution air is low.

Secondly, we conducted simulations on vehicular exhaust diluting continuously in real atmosphere, and found out that BHN can lead to significant NP productions under wide ranges of ambient conditions. BHN is generally favored under low T, high RH, high FSC and ε_s, and low soot concentration. For the conditions investigated in this study, the effect of soot scavenging on NP formation via BHN is significant only when soot particle concentration in the raw exhaust is $>\sim 10^7\,cm^{-3}$. In addition, our model predicts strong sensitivity of H_2SO_4–H_2O nucleation rate to FSC and ε_s. We found that NP formation via BHN may be still possible even if FSC is reduced to ultra-low levels if ε_s is high enough ($\sim$10%). However, if ε_s is around a few percentage, BHN is likely to be negligible in the exhaust of engines running on ultra-low sulfur fuel. The observations of volatile NP formation in such cases (ultra-low FSC) may indicate the involvement of other species such as ions, organics, metal, solid cores or ammonia.

Since NP production via BHN strongly depends on ε_s, measurements of ε_s for motor engines are needed in order to properly assess the contribution of BHN to NP formation in the vehicular exhaust. Simultaneous measurements of nucleated NPs, dilution conditions, FSC and ε_s, and soot emission are needed to better constrain the nucleation model and verify the nucleation mechanisms. Since BHN is very sensitive to FSC (at fixed ε_s), measurements of formed NPs as a function of FSC will also be useful to test the BHN mechanism.

Acknowledgments

This work was supported by the New York State Energy Resource and Development Agency and by the National Science Foundation under grant ATM 0104966.

Appendix A. Calculation of initial H_2SO_4 number concentration and emission index

(1) Calculation of initial H_2SO_4 number concentration in vehicular exhaust before dilution.
The initial $[H_2SO_4]$ in exhaust is calculated based on FSC andε_s and can be expressed as

$$[H_2SO_4] = \frac{FSC \times N_A \times \varepsilon_s \times \rho_{exhaust}}{(1 + AFR) \times M_s}, \qquad (A.1)$$

where N_A is Avogadro constant, AFR is the air fuel ratio which is assumed to be 15 in this study, M_s is the molecular weight of sulfur and $\rho_{exhaust}$ is the density of exhaust.

(2) Calculation of emission index from number concentration of particles larger than 3 nm.
Vehicle NP number emission index (EI, in $\#\,kg^{-1}$ fuel), which could be calculated from $N_{d>3\,nm}$ at the plume age of 1 s, is expressed as

$$EI = N_{d>3\,nm} \times \frac{\text{volume of } e\text{xhaust}}{\text{mass of } f\text{uel}}. \qquad (A.2)$$

Assuming the AFR to be 15, we obtain the volume of exhaust at 1 s (diluted $\sim$700 times in 1 s) as a result of burning 1 kg of fuel, which gives the second term on the right-hand side of the equation.

Appendix B. Supplementary Materials

Supplementary data associated with this article can be found in the online version at doi:10.1016/j.atmosenv.2006.07.012.

References

Bagley, S.T., Baumgard, K.J., Gratz, L.D., Johnson, J.H., Leddy, D.G., 1996. Characterization of fuel and aftertreatment device effects on diesel emissions. Research Report Health Effect Institute 76, 1–75.

Baumgard, K.J., Johnson, J.H., 1996.The effect of fuel and engine design on diesel exhaust particle size distribution. SAE Technical Paper Series, No. 960131.

Donaldson, K., Li, X.Y., MacNee, W., 1998. Ultrafine (nanometer) particle mediated lung injury. Journal of Aerosol Science 29, 553–560.

Doyle, G.J., 1961. Self-nucleation in the sulfuric acid–water system. Journal of Chemical Physics 35, 795–799.

Graves, R.L., 1999. Review of diesel exhaust after treatment programs. SAE Technical Paper Series, No. 1999-01-2245.

Jaecker-Voirol, A., Mirabel, P., Reiss, H., 1987. Hydrates in supersaturated binary sulfuric acid–water vapor: a reexamination. Journal of Chemical Physics 87, 4849–4852.

Kawa, S.R., et al., 1999.Assessment of the effects of high-speed aircraft in the stratosphere:1998. NASA/TP, 2090237.

Kim, D., Gautam, M., Gera, D., 2002. Parametric studies of the formation of diesel particulate matter via nucleation and coagulation modes. Journal of Aerosol Science 33, 1609–1621.

Kim, D.H., Gautam, M., Gera, D., 2001. On the prediction of concentration variations in a dispersing heavy-duty truck exhaust plume using k-epsilon turbulent closure. Atmospheric Environment 35, 5267–5275.

Kittelson, D.B., Kadue, P.A., Scherrer, H.C., Loverien, R.E., 1988. Characterization of Diesel Particle in the Atmosphere. CRC, AP-2 Project Group.

Kittelson, D.B., Winthrop Jr., F.W., Johnson, J.P., 2004. Nanoparticle emissions on Minnesota highways. Atmospheric Environment 38, 9–19.

Kulmala, M., Laaksonen, A., Pirjola, L., 1998. Parameterizations for sulfuric acid/water nucleation rates. Journal of Geophysical Research 103, 8301–8308.

Lukachko, S.P., Waitz, I.A., Miake-Lye, R.C., Brown, R.C., Anderson, M.R., 1998. Production of sulfate aerosol precursors in the turbine and exhaust nozzle of an aircraft engine. Journal of Geophysical Research 103, 16159–16174.

Noppel, M., Vehkamaki, H., Kulmala, M., 2002. An improved model for hydrate formation in sulfuric acid–water nucleation. Journal of Chemical Physics 116, 218–228.

Shi, J.P., Harrison, R.M., 1999. Investigation of ultrafine particle formation during diesel exhaust dilution. Environmental Science and Technology 33, 3730–3736.

Shi, J.P., Harrison, R.M., Evans, D.E., Alam, A., Barnes, C., Carter, G., 2002. A method for measuring particle number emissions from vehicles driving on the road. Environmental Science and Technology 23, 1–14.

Tobias, H.J., Beving, D.E., Ziemann, P.J., Sakurai, H., Zuk, M., McMurry, P., Zarling, D., Waytulonis, R., Kittleson, D.B., 2001. Chemical analysis of diesel engine nanoparticles using a nano-DMA/thermal desorption particle beam mass spectrometer. Environmental Science and Technology 35, 2233–2243.

Yli-Tuomi, T., Aarnio, P., Pirjola, L., Mäkelä, T., Hillamo, R., Jantunen, M., 2005. Emissions of fine particles, NO_x, and CO from on-road vehicles in Finland. Atmospheric Environment 39, 6696–6706.

Yu, F., 2001. Chemiions and nanoparticles formation in diesel engine exhaust. Geophysical Research Letters 28, 4191–4194.

Yu, F., 2005. Quasi-unary homogeneous nucleation of H_2SO_4–H_2O. Journal of Chemical Physics 122, 074501.

Yu, F., 2006. Binary H_2SO_4–H_2O homogeneous nucleation rates based on a kinetic quasi-unary model: look-up tables. Journal of Geophysical Research 111, D04201.

Zhang, K.M., Wexler, A.S., 2004. Evolution of particle number distribution near roadways-Part I: analysis of aerosol dynamics and its implications for engine emission measurement. Atmospheric Environment 38, 6643–6653.